

# Corrosion behaviour of Al<sub>86.0</sub>Co<sub>7.6</sub>Ce<sub>6.4</sub> glass forming alloy with different microstructures



C.L. Li<sup>a,\*</sup>, P. Wang<sup>a</sup>, S.Q. Sun<sup>a</sup>, K.T. Voisey<sup>b</sup>, D.G. McCartney<sup>b</sup>

<sup>a</sup> Department of Materials Physics and Chemistry, College of Science, China University of Petroleum (East China), Qingdao 266580, PR China

<sup>b</sup> Materials, Mechanics and Structures Research Division, Faculty of Engineering, The University of Nottingham, Nottingham NG7 2RD, UK

## ARTICLE INFO

### Article history:

Received 6 February 2016

Received in revised form 12 April 2016

Accepted 30 April 2016

Available online 9 May 2016

### Keywords:

Al-Co-Ce

Glass forming alloy

Microstructure

Corrosion behaviour

## ABSTRACT

It has been extensively reported that Al-TM-RE amorphous alloy has excellent mechanical properties and corrosion resistance. In this paper, the corrosion behaviour of an Al<sub>86.0</sub>Co<sub>7.6</sub>Ce<sub>6.4</sub> glass forming alloy with different microstructures is investigated through electrochemical experiments and microscopy. Results show the effect of microstructure. Laser and electron beam surface melting processes produce rapidly solidified microstructures with different extents of passivation compared to the as-cast alloy. An amorphous surface layer produced by these surface treatments had superior corrosion resistance compared with the crystalline alloy. As-cast and laser treated Al<sub>86.0</sub>Co<sub>7.6</sub>Ce<sub>6.4</sub> suffered localised corrosion in the Al/Al<sub>11</sub>Ce<sub>3</sub> eutectic region whereas the amorphous material exhibited uniform corrosion. Compared with the electrochemical behaviour of AA2024 and Alclad 2024, the fully amorphous layer prepared by combined laser-electron beam treatment exhibited advantages such as the more negative corrosion potential, the higher pitting potential and the uniform corrosion mechanism, which indicates that this material is a potential anode candidate in the protection of AA2024.

© 2016 Elsevier B.V. All rights reserved.

## 1. Introduction

High strength aluminium alloys are a family of commercial aeronautical alloys. However, these alloys are susceptible to various types of local corrosion including pitting, inter granular corrosion, exfoliation corrosion and stress corrosion cracking [1,2]. To date, many corrosion prevention methods have been developed and applied for these aluminium alloys such as cladding [3], anodising [4,5], corrosion inhibitors [6,7], and conversion coatings [8,9], etc. Each of these methods has different corrosion prevention mechanisms and drawbacks. For instance, alclad layers usually have limited protection distance when the layers are scratched, and chromate conversion coatings have been gradually phased out due to the toxicity to the environment and carcinogenicity to human beings [10]. A new environmentally friendly, good corrosion resistant, long-lifespan corrosion prevention method is therefore desired.

Because of the highly different microstructure compared to the crystalline alloy, and its favourable properties, the amorphous alloy has attracted enormous attention and stimulated widespread research enthusiasm. Al-TM-RE (TM = transition metal, RE = rare

earth) alloys are one of most interested families of amorphous alloy due to their outstanding mechanical properties [11,12] and corrosion resistance [13]. The favourable corrosion resistance of the Al-TM-RE amorphous alloys is attributed to their three instincts. First, the lack of defects such as grain boundaries, dislocations and precipitates makes these amorphous alloys a good barrier to prevent local corrosion. Second, their open circuit potential (OCP) is tunable with the concentration of TM and RE elements [14]. It has been reported that when the suitable chemical composition was used, the OCP of alloy could be hundreds of millivolt lower than AA2024, which indicates that the amorphous alloy could be used as an anode in the protection of AA2024. Third, these amorphous alloys can provide active inhibition through releasing corrosion inhibitors such as Ce<sup>3+</sup>, Y<sup>3+</sup> and Gd<sup>3+</sup> ions which are good to protect aluminium alloys [15].

In this context, a new coating system with the Al-TM-RE nanocrystalline/amorphous layer substituting the conventional roll-bonded cladding layer in the protection of high strength aluminium (such as AA2024) has been proposed [16]. Based on electrochemical tests and salt fog tests, Al-TM-RE nanocrystalline/amorphous layer was proven to have favourable corrosion resistance [17,18]. More relevant to the current work, our previous work has demonstrated that an amorphous surface layer can be generated in these alloys (Al-Co-Ce glass forming alloy) via electron beam surface treatment [19]. It has also been shown

\* Corresponding author.

E-mail addresses: [lichunling@upc.edu.cn](mailto:lichunling@upc.edu.cn), [chunling.li@outlook.com](mailto:chunling.li@outlook.com) (C.L. Li).

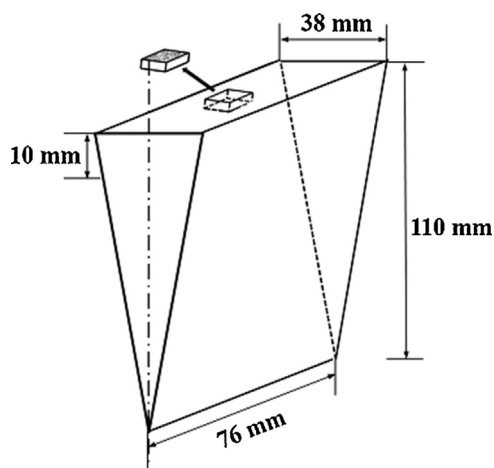


Fig. 1. Dimensions of the as-cast Al-Co-Ce alloy ingot.

that the electron beam treated material has a superior corrosion behaviour compared to the as-cast alloy, however this is limited by the presence of cracks through the amorphous layer [20]. A prior laser surface treatment to refine the microstructure was shown to increase the ease of amorphisation as well as to decrease the extent of cracking [21]. In order to develop the understanding of microstructure-corrosion behaviour relationship of Al-TM-RE nanocrystalline/amorphous alloy, the corrosion behaviour of Al-Co-Ce glass forming alloys with different microstructures was therefore studied in the present work, including coarse-grain crystalline alloy, microstructure refined crystalline alloy, cracked amorphous layer and crack-free amorphous layer. These four microstructures mentioned above correspond to as-cast alloy, laser surface remelted (LSM) alloy, electron beam surface remelted (EBSM) alloy and laser-electron beam surface remelted (LSM-EBSM) alloy, respectively. Corrosion mechanisms of different materials are discussed and schematically illustrated. In addition, AA 2024 and alclad 2024 are used as reference materials, as well as pure Al, to study the possibility of LSM-EBSM treated Al-Co-Ce amorphous layer replacing the cladding layer on AA2024 by comparing their corrosion morphology and electrochemical behaviour.

## 2. Materials and experimental methods

### 2.1. Materials and microstructural characterisation

In this work, corrosion behaviour of  $\text{Al}_{86.0}\text{Co}_{7.6}\text{Ce}_{6.4}$  (at.%) alloy with four different types of microstructures was investigated, including as-cast sample, laser surface remelted (LSM) sample, pulsed electron beam surface remelted (EBSM) sample and the sample treated with both laser and electron beam (LSM-EBSM). For the as-cast sample, Al, Co and Ce lumps with a size of approximately  $10 \times 10 \times 10$ ,  $5 \times 5 \times 2$  and  $3 \times 3 \times 3$  mm, respectively, were melted in a magnesia crucible through an induction heating coil and then cast in a wedge-shaped steel mould under an argon atmosphere. Prior to melting and casting, the crucible and the mould were located in an air-free (air pressure was  $<10^{-3}$  mbar) and argon refilled (argon pressure was 500 mbar) environment. The required pouring temperature for Al-Co-Ce alloys was  $1100^\circ\text{C}$ . A holding time of 30 min at the pouring temperature was allowed to ensure complete melting and homogenisation of the melt before pouring. After casting, the ingot together with the mould were retained in the argon atmosphere to cool down for 30 min, in order to avoid oxidation. The dimensions of the ingot are shown in Fig. 1. The samples used in this work, including corrosion test, laser or electron beam treatment, were taken from the middle of the ingot with

the distance of less than 10 mm from the top surface as shown in Fig. 1.

For the LSM sample, it was derived from the laser surface remelting treatment of the as-cast sample as above mentioned using a fibre laser (IPG laser, GmbH, Germany). The detailed information of the laser machine and treatment parameters can be found in our previous work [21]. A PIKA electron beam surface finishing machine (PF32A) developed by Sodick, Japan was used to prepare EBSM sample. The detailed information of this machine and the parameters of electron beam surface treatment were described in Walker's work [22] and our published paper [19,21], respectively. In particular, the LSM-EBSM sample was fabricated with a prior laser surface remelting and a following electron beam surface treatment [21]. Details of samples preparation and alloy microstructures are summarised in Table 1.

A FEI XL30 environmental scanning electron microscope with a field emission gun with 20 kV acceleration voltage and  $\sim 10$  mm working distance was used to observe the alloy microstructure. In this work, X-ray diffraction (XRD) was used to investigate the phases present and qualitative phase fraction present in different samples. For bulk materials i.e. as-cast sample, normal X-ray diffraction (XRD) analysis was used. XRD was conducted using a Siemens D500 X-ray diffractometer ( $\text{CuK}\alpha$ ) with a step size of  $0.02^\circ$  and a counting time per step of 2 s. After LSM, EBSM and LSM-EBSM treatment, there is a microstructural transformed layer on the top surface of the treated material. To analyse the outer, treated layer in isolation, glancing angle XRD (GAXRD) using a Bruker D8 Advance diffractometer ( $\text{CuK}\alpha$ ) was carried out. In this work, GAXRD patterns were collected with a step interval of  $0.02^\circ$ , a dwell time of 8 s and a  $2^\circ$  angle of incidence.

AA2024 and alclad 2024 were also used as reference materials to evaluate the corrosion performance of Al-Co-Ce alloy. Prior to corrosion testing, for the macroscopic examination of AA2024 and alclad 2024 samples, a Nikon optical microscope together with ACT-1 software was used in this work. The samples were etched by Keller's reagent (a mixture of 95 mL distilled water, 2.5 mL  $\text{HNO}_3$ , 1.5 mL  $\text{HCl}$  and 1.0 mL  $\text{HF}$ ) for 2 min at room temperature. Fig. 2 shows the optical image of reagent etched AA2024 alloy and alclad 2024, respectively. The compositions of AA2024 alloy and alclad 2024 are listed in Table 2.

### 2.2. Corrosion testing

#### 2.2.1. Sample preparation

In this work, the corrosion behaviour of Al-Co-Ce alloy with different microstructures was investigated through potentiodynamic polarisation testing and corrosion morphologies observation. In addition, corrosion tests of pure Al, AA2024 and alclad 2024 were also performed to allow the comparison of corrosion behaviour. These samples were prepared into working electrodes.

For the as-cast Al-Co-Ce sample, AA2024 and alclad 2024, they were first mounted using non conductive resin then wet polished with  $6\text{ }\mu\text{m}$  diamond paste,  $1\text{ }\mu\text{m}$  diamond paste and  $0.05\text{ }\mu\text{m}$  silica suspensions, in turn. After drying, the mounted samples were electrically connected with a threaded brass rod through the back of the resin. In order to eliminate the occurrence of crevice corrosion between samples and the resin, the edges of samples were lacquered. The exposed area in this type of electrode was  $\sim 1\text{ cm}^2$ .

For the laser or electron beam treated Al-Co-Ce alloy, it was impossible to prepare the working electrodes in the same way as the as-cast materials and AA2024 alloy due to the size limit imposed by cracking. An alternative method was used. The samples were first clamped into a metallic crocodile clip which is connected with a conducting wire to the potentiostat. The crocodile clip has a plastic cover which can prevent its main body from the corrosion solution. At the mouth of the clip, apart from the required exposed

Download English Version:

<https://daneshyari.com/en/article/5354117>

Download Persian Version:

<https://daneshyari.com/article/5354117>

[Daneshyari.com](https://daneshyari.com)